

ChartAgent: A Chart Understanding Framework with Tool Integrated Reasoning

Boran Wang^{*§}, Xinming Wang^{†‡§}, Yi Chen^{†‡§}, Xiang Li[¶], Jian Xu^{†‡}, Jing Yuan^{*}, Chenglin Liu^{†‡}

^{*}College of Artificial Intelligence, Nankai University, Tianjin 300350, China

[†]University of Chinese Academy of Sciences, Beijing 100049, China

[‡]State Key Laboratory of Multimodal Artificial Intelligence Systems (MAIS),
Institution of Automation, Chinese Academy of Sciences, Beijing 100190, China

[§]Zhongguancun Academy, Beijing 100094, China

[¶]State Key Laboratory for Novel Software Technology, Nanjing University, Nanjing 210023, China

Abstract—With their high information density and intuitive readability, charts have become the de facto medium for data analysis and communication across disciplines. Recent multimodal large language models (MLLMs) have made notable progress in automated chart understanding, yet they remain heavily dependent on explicit textual annotations and the performance degrades markedly when key numerals are absent. To address this limitation, we introduce ChartAgent, a chart understanding framework grounded in Tool-Integrated Reasoning (TIR). Inspired by human cognition, ChartAgent decomposes complex chart analysis into a sequence of observable, replayable steps. Supporting this architecture is an extensible, modular tool library comprising more than a dozen core tools—such as key-element detection, instance segmentation, and optical character recognition (OCR)—which the agent dynamically orchestrates to achieve systematic visual parsing across diverse chart types. Leveraging TIR’s transparency and verifiability, ChartAgent moves beyond the black-box paradigm by standardizing and consolidating intermediate outputs into a structured Evidence Package, providing traceable and reproducible support for final conclusions. Experiments show that ChartAgent substantially improves robustness under sparse-annotation settings, offering a practical path toward trustworthy and extensible systems for chart understanding.

I. INTRODUCTION

Charts have become indispensable to scientific research and business analytics as a universal medium for condensing data and conveying insights Wang et al. [2023]. By presenting latent patterns and relationships in complex data with intuitive, high-information-density encodings, charts are among the most prevalent visualization methods in scientific literature and business reports. This widespread reliance, in turn, creates an urgent demand for automated chart understanding. In recent years, MLLMs Team et al. [2023] Wang et al. [2024] Liu et al. [2023c] have markedly advanced automated chart understanding, demonstrating strong capabilities in chart question answering, chart conversion, and data summarization. However, experiments reveal that the success of current MLLMs is highly dependent on the rich and explicit text annotations present within the chart images. Fig.1 (a) presents the performance of mainstream MLLMs on both annotated and unannotated charts from the ChartBench dataset Xu et al. [2023]. It is evident that these models, once successful with textual cues, experience a drastic performance decline when

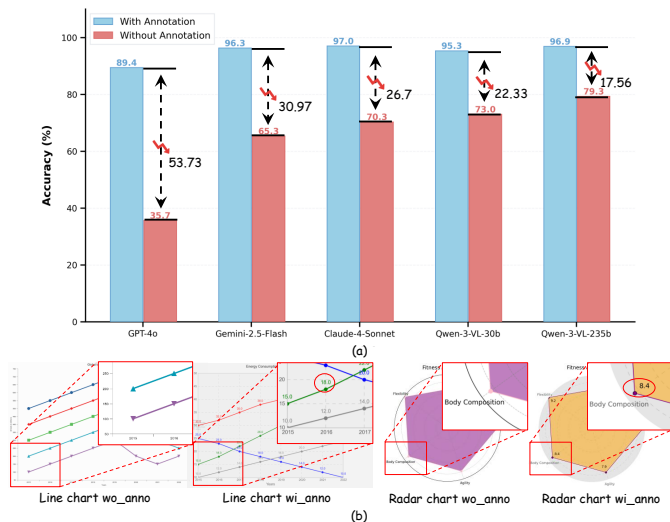


Fig. 1. (a) presents the accuracy of mainstream MLLMs in answering numerical question-answering tasks on both annotated and unannotated charts. A significant decline in accuracy is observable across all models. (b) demonstrates the distinctions between the different types of annotated and unannotated charts within the ChartBench dataset. Specifically, the annotated charts feature precise numerical labels at key positions (as indicated by the content within the red circles).

facing real world scenarios with missing or sparse key numerical information, thereby struggling to perform accurate visual reasoning and data extraction. Specifically, GPT-4o Hurst et al. [2024] exhibits an accuracy difference of 53.73% when answering numerical questions on annotated versus unannotated charts. Even Qwen3-VL Bai et al. [2025], the model least affected, observe accuracy decline by 17.56 p.p.

This vulnerability profoundly reveals the limitations of current mainstream end-to-end models in deep visual information understanding. Most MLLMs tend to treat chart understanding as a black-box mapping from raw pixels directly to textual answers, lacking structured, verifiable intermediate visual representations and elements recognition steps Huang et al. [2025a]. When textual cues are insufficient, the models struggle to revert to more fundamental visual evidence (such as line chart inflection point coordinates, pie chart sector

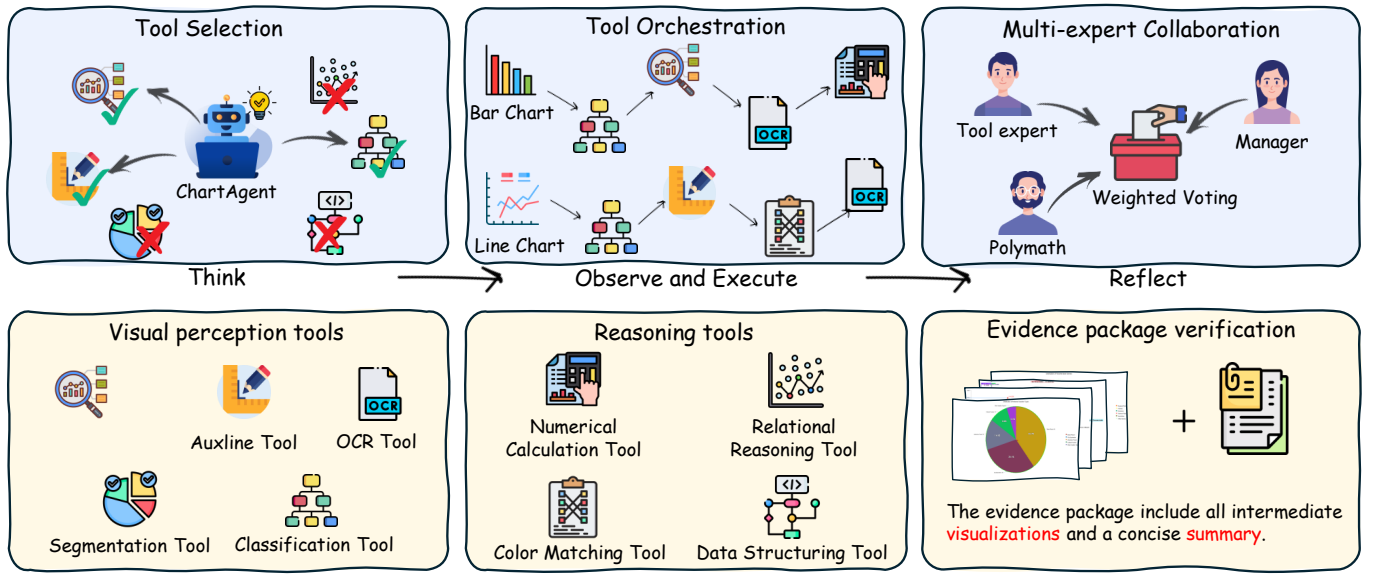


Fig. 2. The figure illustrates ChartAgent’s complete Think-Observe-Execute-Reflect process. The toolkit, comprising both visual perception tools and reasoning tools, support the entire process cycle of ChartAgent. The constructed evidence package subsequently offers the necessary basis for post-hoc verification.

angles, etc.), thereby failing to autonomously perform reliable numerical inferences Huang et al. [2024]. More critically, this opaque reasoning paradigm undermines the traceability of the decision-making path: even when an answer is provided, researchers find it difficult to verify its basis, which consequently constrains the scalable deployment and application of chart understanding in precision-sensitive scenarios such as scientific research and finance.

In contrast, human analysts adhere to a highly structured cognitive process when interpreting charts: they do not comprehend the entire image at a single glance Salamatian et al. [2025], but instead adopt a decomposed and instrumentalized strategy. This involves first identifying the axes and legend, then reading the scales and labels, subsequently locating the relevant data markers based on the specific question, and completing numerical mapping through visual measurement, ultimately integrating multi-source information for calculation and reasoning. The entire procedure is step-by-step, systematic, and evidence-based.

Inspired by the human analytical process, this paper aims to overcome the core limitations of current MLLMs in comprehending charts, and proposes a chart understanding agent framework ChartAgent, based on Tool-Integrated Reasoning (TIR) Lin and Xu [2025]. Its core idea is to transform complex chart analysis tasks from an end-to-end black-box mapping into a reasoning chain composed of programmable steps that are observable and controllable. To support this architecture, we construct an extensible modular tool library comprising over a dozen visual and reasoning tools. ChartAgent serves as an intelligent scheduling hub, dynamically orchestrating and invoking these tools based on user queries to perform in-depth chart parsing in systematically, thereby significantly reducing reliance on textual annotations. Our main contributions are as

follows:

- We propose a new chart-understanding agent framework, ChartAgent. The framework decomposes complex chart-reading tasks into a sequence of observable and replayable intermediate steps and dynamically orchestrates tools under a cost–gain trade-off, yielding a transparent, interpretable, and verifiable reasoning chain that provides solid evidential support for reliable conclusions.
- A dedicated modular tool library for chart understanding is constructed. It comprises over a dozen tools, which are orchestrated and invoked by the agent. The intermediate results output by these tools are aggregated into standardized evidence packages, supporting the verifiability and robustness of the final answers.
- ChartAgent achieves state-of-the-art(SOTA) performance with traceable interpretations across NumberQA(NQA), Value Compare, and chart-to-table tasks on the ChartQA and ChartBench datasets.

II. RELATED WORK

A. MLLMs for Chart Understanding

Represented by GPT Achiam et al. [2023], Gemini Team et al. [2023], and QwenVL Bai et al. [2023], general MLLMs exhibit strong zero-shot visual reasoning owing to pre-training on massive image–text pairs. However, for chart understanding tasks that demand higher precision and stronger domain-specific priors, they remain inadequate. Their primary limitation is a text-first reasoning paradigm that over-relies on explicit textual cues in charts (e.g., legends and data labels). In addition, the patch-based visual representations Han et al. [2022] and aggregation mechanisms commonly employed by these models are intrinsically weak in geometric perception and in detecting subtle, continuous scale differences, making

it difficult to support axis-scale mapping and fine-grained geometric measurements of length and angle. These factors collectively constrain their utility and reliability in chart understanding.

B. Domain-specific Chart Models

To address the foregoing limitations, researchers explore domain-specific chart models. Early works such as Donut Kim et al. [2022] and Pix2Struct Lee et al. [2023], which are end-to-end, OCR-free visual document understanding models, lay the groundwork for subsequent generative methods. Recent works improve chart-text alignment and refine fine-grained reasoning pipelines to enhance MLLMs’ chart understanding Chen et al. [2024]. For example, MatCha Liu et al. [2023b] and UniChart Masry et al. [2023] augment the Pix2Struct and Donut frameworks, respectively, with chart-specific pre-training tasks—such as MatCha’s “chart de-rendering” and UniChart’s numerical reasoning—to better capture chart structure and underlying data. ChartAssistant Meng et al. [2024] and ChartMoE Xu et al. [2024] tackle the problem through task decomposition and architectural design: the former argues that general MLLMs lack structured knowledge and therefore introduces chart-to-table pre-training to strengthen the alignment between visual elements and data substantially; the latter contends that a single connector cannot accommodate the diversity of chart-understanding tasks, adopting a mixture-of-experts (MoE) framework Shazeer et al. [2017] and training specialized experts with more diverse alignment objectives (e.g., chart-to-JSON, chart-to-code) to improve generalization. Works such as MMCA Liu et al. [2024] and ChartInstruct Masry et al. [2024] likewise employ differentiated alignment strategies to further strengthen the model’s grasp of chart content.

On the other hand, a line of work focuses on making the reasoning chain explicit and controllable. For example, TinyChart Zhang et al. [2024] adopts Program-of-Thoughts (PoT) to strengthen numerical reasoning, while ChartSketcher Huang et al. [2025b] draws on human cognitive processes by introducing Sketch-CoT, enabling the model to annotate charts with sketch-like markings to obtain multimodal feedback and iteratively correct its visual understanding. Although such models achieve notable performance gains via domain-specific fine-tuning, they remain fundamentally end-to-end black-box systems with the decision pathways opaque and difficult to verify. Consequently, in scenarios with sparse textual annotations and a need for precise visual measurements, their robustness and trustworthiness remain constrained.

C. Agent Frameworks with Tool Use

In parallel with end-to-end fine-tuning, the LLM-based agent paradigm Wang et al. [2025] Gupta and Kembhavi [2023], often referred to as tool augmentation, has gained traction Du et al. [2024]. Inspired by ReAct Yao et al. [2022], agents decompose complex tasks into an iterative think-act-observe loop Schick et al. [2023], so as to decouple perception from reasoning: the model delegates verifiable

operations to external tools and incorporates environmental feedback to compensate for large models’ limitations in precise perception and retrieval. In chart-centric scenarios, prior approaches typically invoke specialized models such as DePlot Liu et al. [2023a] and StructChart Xia et al. [2023] to transduce images into structured representations (e.g., tables or JSON as low-level data), then linearize these structures into text for a LLM to perform higher-level analysis and generate answers.

III. CHARTAGENT

A. Overall Framework

ChartAgent adopts a training-free, zero-shot paradigm with cognition-inspired, tool-integrated reasoning that decomposes complex chart parsing into a sequence of controllable, replayable steps. As shown in Fig. 2, the agent first ingests the chart image and task instruction, performs chart-type recognition and subtask decomposition, and then dynamically orchestrates the appropriate tools according to the chart type and task to progressively extract structural and semantic information. The intermediate results produced by each tool are consolidated into an evidence package, rendering the entire reasoning chain transparent, traceable, and verifiable. In the final decision stage, a GroupTalk-based multi-expert collaboration mechanism conducts consensus voting and confidence fusion over the outputs from multiple tools, producing the final answer together with a structured analysis. Leveraging the curated tool library and the large language model, the entire pipeline requires no additional training to achieve automated understanding and information extraction for complex charts.

B. Modular Tool Library Construction

To better perform chart understanding tasks, we develop an extensible, chart-oriented tool library comprising more than a dozen core capabilities, endowing the agent with two classes of functions: low-level visual perception and high-level reasoning/integration. The visual tools provide fundamental sensing—element detection, region segmentation, text recognition, and geometric measurement—while the reasoning tools undertake higher-level analysis such as numerical computation, relational modeling, and data structuring. A complete inventory of tools and additional visualization examples are provided in the Appendix.

As illustrated in the upper panel of Fig. 3, when a sector-type chart is given as input, ChartAgent first invokes the `ChartClassificationTool` to determine the chart type, thereby planning subsequent tool selection and orchestration. After the tools are selected, it calls the `SegmentationTool` to extract regions of interest and, together with the `SegmentationAugmentTool` tailored for pie and ring charts, performs sector-level instance segmentation. Once sufficient low-level visual evidence has been obtained, ChartAgent employs reasoning tools such as `NumericalCalculationTool` and `DataStructuringTool` to conduct numerical estimation, metric aggregation, and structured organization, thereby correctly answering a question

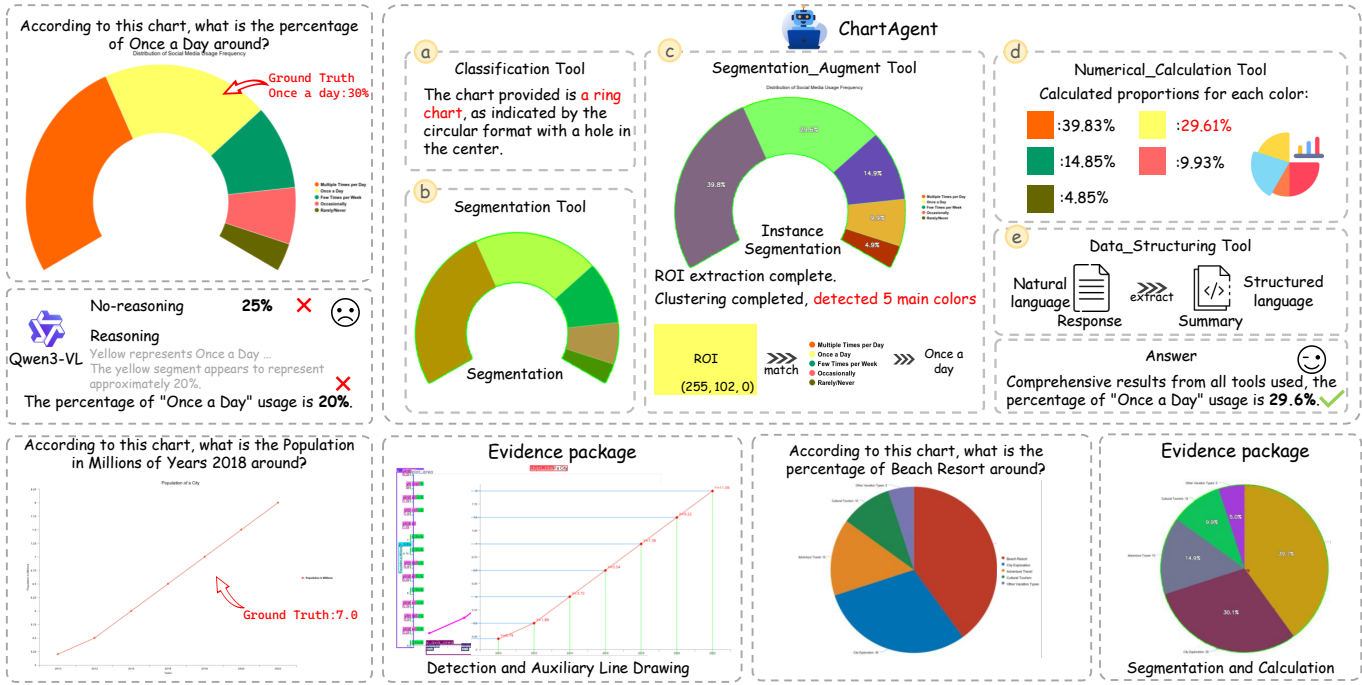


Fig. 3. Two distinct chart processing scenarios are showcased. The upper panel details the tool selection and orchestration by ChartAgent when handling a sector chart lacking explicit text annotations, further displaying the intermediate results generated by each utilized tool. The lower panel showcases the resulting visualization output of the evidence package when the ChartAgent processes a line graph without annotations.

previously answered incorrectly by Qwen3-VL and producing an evidence package for verification. The lower panel of Fig. 3 showcases other representative visual tools. For line and scatter charts, the AuxLineDrawerTool leverages detected key elements to automatically draw auxiliary lines, robustly mapping data points to axis ticks and generating verifiable visual evidence. The KeyElementDetectionTool detects axes, ticks, legends, and series markers to supply reliable priors for subsequent measurement and alignment. Several tools are implemented atop mature vision models, such as YOLO Khanam and Hussain [2024] Jocher et al. [2023] and SAM Kirillov et al. [2023] Ravi et al. [2024], to establish a robust perceptual foundation.

Beyond the visual perception layer, the library also contains a set of reasoning and structuring tools to post-process and consolidate raw perceptual outputs. NumericalCalculationTool performs fundamental operations such as summation, normalization, ratio conversion, and logical evaluation; RelationalReasoningTool constructs semantic and spatial relation graphs among elements based on detection and segmentation, enabling interval comparison, trend analysis, and cross-series alignment; DataStructuringTool integrates fragments from OCR, detection, and computation into standardized tables or JSON so that the agent can execute final structured queries and explanations. The two classes of tools are mutually reinforcing, enabling the agent to complete a human-like “think–observe–act–reflect” chart-reading loop. All tools adhere to a unified interface schema that standardizes

function descriptions, parameters, and meta-information (e.g., cost estimates and expected information gain). Building on this schema, ChartAgent performs a cost–information-gain trade-off to dynamically select the optimal tool sequence and commits outputs from each stage to a structured evidence package, thereby supporting subsequent consistency checks and auditable verification.

C. Dynamic Tool Orchestration

Before ChartAgent organizes multi-step reasoning via a function-calling mechanism, we inject the aforementioned tool interfaces and meta-information into the system prompt so that the model is aware of each tool’s functionality, parameters, and invocation cost. During iterative reasoning, the LLM emits a structured directive—either a `<tool_call>` containing the tool name, parameters, and rationale, or a `<finish>` that terminates the reasoning. Upon receiving a `<tool_call>`, the agent validates the tool name and parameter legality, checks invocation quotas and call limits, executes the tool, and commits its outputs to an internal evidence package. When a `<finish>` is received, the agent halts iteration, aggregates the available perceptual evidence, and proceeds to finalization. If the LLM produces unparseable or unexpected output, the system records a log and continues iterating under constraints to keep the process stable and controllable. Overall, the workflow follows a classic think–observe–act–reflect loop: the LLM undertakes decision-making and logical inference, while the tools interact with the external environment and supply verifiable observational evidence; together, they accomplish complex chart understanding.

To enable efficient and stable orchestration, the agent maintains two key caches: state and history. The state cache records concise summaries of each tool—for example, element categories and counts detected by detection tools, mask area ratios obtained from segmentation, and coordinate readings produced by auxiliary-line mappings. After compression and filtering, only salient information is retained to control prompt length and reasoning cost. The history cache logs, for every iteration, the invoked tool’s name, parameters, result summary, and call order, which supports decision tracing and error analysis while facilitating subsequent provenance tracking and verification. When constructing the next-round prompt, the system embeds the accumulated state and a pruned history so that the LLM is aware of the available information and the steps already completed, while also injecting quota reminders and cost-control policies (e.g., calls already made and recommended limits) to guide more cautious and effective decisions under a cost–information gain trade-off. Through these mechanisms, the control layer achieves fine-grained scheduling over the reasoning process, ensuring the validity and rationality of tool invocations while avoiding unnecessary repetition.

In practice, the agent typically first invokes a `ChartClassification` tool to determine the chart type, and then selects the corresponding tools to progressively acquire structured information. Once the evidence is sufficient and the answer is verifiable, the LLM outputs `<finish>` to terminate the iteration. If the reasoning process reaches the maximum number of rounds without convergence, the system forcibly enters the `<finish>` phase and triggers a fallback strategy: it returns the currently accumulated intermediate results and the evidence package, explicitly marking any incompleteness, thereby ensuring that a usable and auditable response is produced under all circumstances.

The foregoing description outlines the tool-invocation workflow from a system implementation perspective. To formalize this decision process at the computational level, we model it as a partially observable decision problem.

a) Computational formalization.: Let the chart image and instruction be (x, q) and the answer variable be $Y \in \mathcal{Y}$. At round t , the agent has accumulated evidence E_t and maintains a belief $b_t(y) = \Pr(Y = y \mid E_t, x, q)$ with entropy $H(b_t) = -\sum_{y \in \mathcal{Y}} b_t(y) \log b_t(y)$. $H(\cdot)$ denotes the Shannon entropy. The action space is $\mathcal{A} = \mathcal{T} \cup \{\text{finish}\}$, where \mathcal{T} is the set of callable tools with nonnegative invocation cost $c(a) \geq 0$ for $a \in \mathcal{T}$. Invoking a tool a produces a stochastic observation Z_a drawn from

$$Z_a \sim p(\cdot \mid a, E_t, x, q), \quad (1)$$

$$b_{t+1}^{(a,z)}(y) = \Pr(Y = y \mid E_t, a, z, x, q). \quad (2)$$

b) Myopic decision rule under a cost-gain trade-off.: We score each tool by its expected information gain (EIG), written compactly as a conditional mutual information:

$$\begin{aligned} \text{EIG}_t(a) &= I(Y; Z_a \mid E_t, x, q) \\ &= H(b_t) - \mathbb{E}_{z \sim p(\cdot \mid a, E_t, x, q)} \left[H\left(b_{t+1}^{(a,z)}\right) \right]. \end{aligned} \quad (3)$$

A one-step lookahead policy chooses

$$a_t = \arg \max_{a \in \mathcal{T}} \left\{ \text{EIG}_t(a) - \lambda c(a) \right\}, \quad (4)$$

where $\lambda > 0$ balances information gain against cost. A budget B enforces $\sum_{s=1}^t c(a_s) \leq B$. We terminate when

$$\max_{a \in \mathcal{T}} \left\{ \text{EIG}_t(a) - \lambda c(a) \right\} \leq \eta \quad \text{or} \quad \sum_{s=1}^t c(a_s) \geq B, \quad (5)$$

with threshold $\eta \geq 0$, and then produce the final decision based on b_t together with the evidence package.

D. Multi-Expert Collaboration

ChartAgent introduces a multi-expert collaboration mechanism at the decision stage to simulate multi-party deliberation and enhance reliability and robustness under uncertainty. Concretely, we preset several experts with complementary foci who share the same historical state but emphasize different evidence dimensions: a tool expert evaluates the rationality of each tool invocation and the quality of its outputs, while a synthesis expert concentrates on integrating cross-source cues and performing consistency checks. When arbitration is required (e.g., conflicting results or dispersed confidences), each expert independently issues a vote with a score and a confidence estimate based on the current image and accumulated state. The votes are then aggregated and calibrated—performing score normalization and confidence re-scaling—and, when necessary, thresholds and temperature parameters are applied to select the top-scoring candidate as the final decision, with optional remedial invocations or additional verification triggered by rule to mitigate the risk of error.

As a pluggable decision-enhancement module, GroupTalk can be inserted at key nodes of the main reasoning loop, including tool selection (e.g., prioritizing between key-element detection and direct OCR), conflict resolution (arbitrating or triggering re-validation when tools disagree), and result fusion (weighted integration across sources or selection of the highest-confidence conclusion). This mechanism injects “collective intelligence” into ChartAgent, substantially improving robustness and transparency under complex and noisy conditions. The rationales, confidence scores, and cited evidence for all ballots—together with the aggregation and arbitration procedures—are logged step-by-step into the evidence package to form an auditable decision trail, facilitating post-hoc traceability and human verification.

E. Evidence Package Verification

To enable verifiable reasoning, ChartAgent introduces a chart evidence package (CEP) mechanism at the output stage. The CEP systematically aggregates key intermediate artifacts generated throughout the pipeline—including detected bounding boxes with visualization overlays, OCR-extracted text with coordinates, segmentation masks, color statistics and comparative results, auxiliary-line alignment diagrams, and GroupTalk voting and arbitration logs and archives them in a structured

TABLE I
PERFORMANCE OF CHARTAGENT AND PRIOR METHODS ON CHARTBENCH. RELAXED ACCURACY (%) FOR THE NUMBERQA (NQA) TASK AND ACCURACY (%) FOR THE VALUE COMPARE (VC) TASK ARE REPORTED FOR CHART-SPECIFIC MODELS AND GENERAL-PURPOSE MLLMS.

ChartBench					
NumberQA (NQA)			Value Compare (VC)		
Chart Models	Relax Acc.	General MLLMs	Relax Acc.	General MLLMs	Acc.
MatCha	25.86	GPT-4o	45.33	GPT-4o	65.42
UniChart	27.44	Gemini-2.5 Flash	63.26	Gemini-2.5 flash	84
ChartMoE	51.67	Claude4	63.86	Claude4	78.32
ChartVLM	32.19	Qwen2.5VL-72b	63.11	Qwen2.5VL-72b	79.61
ChartLlama	21.31	Qwen3VL-30b	63.81	Qwen3VL-30b	66.57
TinyChart	47.86	CharAgent(Qwen3vl-30b)	68.46(↑4.65)	ChartAgent	69.78(↑13.21)
ChartGemma	38.46	Qwen3VL-235b	71.48	Qwen3VL-235b	82
ChartInstruct	31.75	CharAgent(Qwen3vl-235b)	73.25(↑1.77)	ChartAgent	84.57(↑12.57)

format with indices and concise summaries, providing traceable support for the final answer. With the CEP, ChartAgent is no longer an inscrutable black box: users and researchers can replay the reasoning trajectory step by step to verify that each operation is evidence-based, thereby substantially improving interpretability and trustworthiness. For example, when answering “What is the value for a specific year in the line chart?”, the CEP presents the localization of the year label, screenshots and readings from auxiliary-line-to-axis-tick mappings, and the corresponding text-extraction results, making the evidential basis of the answer explicit. The CEP likewise facilitates error diagnosis: if the final conclusion deviates, developers can quickly pinpoint the faulty tool or stage, providing direct cues for subsequent fixes and system improvements. Overall, this mechanism renders the reasoning process explicit and replayable, enabling traceable, evidence-grounded question answering and laying the groundwork for deployment in high-reliability settings.

IV. EXPERIMENT

A. Dataset and Evaluation Metrics

a) *Dataset*: We systematically evaluate ChartAgent on two public chart-understanding datasets, ChartBench Xu et al. [2023] and ChartQA Masry et al. [2022]. ChartBench targets charts with sparse textual annotations and spans 9 major categories and 42 subcategories; on this dataset, we focus on two relatively challenging tasks: NumberQA(NQA) and Value Compare. The ChartQA test set contains 1,250 question-answer pairs, with questions divided into Human and Augmented subsets. It covers the three most common chart types, and all charts originate from real-world scenarios. On ChartQA, we evaluate both chartQA and the chart-to-table conversion task.

b) *Evaluation Metrics and Implementation Details*: Similar to Wei et al. [2025] Yang et al. [2024], we adopt relaxed accuracy for NQA to better reflect practical tolerance in chart reading, and standard accuracy for Value Compare. For the chart-to-table task, we follow Liu et al. [2023a] and report the RMS_{F1} metric to ensure comparability with prior work. In this section, all ChartAgent variants adopt

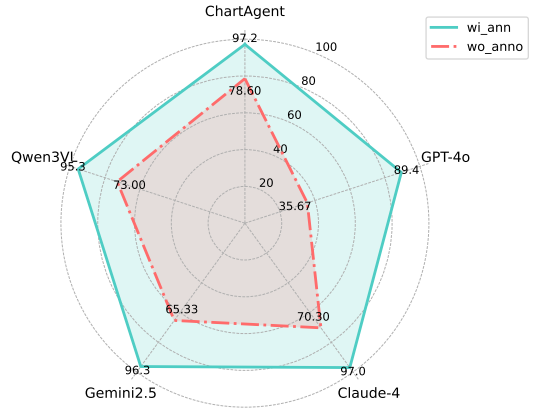


Fig. 4. Accuracy (%) of MLLMs and ChartAgent on charts with explicit numerical annotations (With ann) and on de-annotated charts without such labels (Without ann).

Qwen3VL as the base model. ChartAgent(Qwen3VL-30B) and ChartAgent(Qwen3VL-235B) denote the model-driven agent variants instantiated with the 30B and 235B base models, respectively.

B. Performance Comparison

a) *ChartBench*: As shown in Table I, on the ChartBench dataset ChartAgent demonstrates outstanding performance. For NQA, the lenient accuracy of the 30B and 235B variants reaches 68.46% and 73.25%, respectively—surpassing all compared domain-specialized chart models (ChartMoE, 51.67%; TinyChart, 47.86%) and exceeding their corresponding baselines Qwen3-VL-30B (63.81%) and Qwen3-VL-235B (71.48%) by 4.65 and 1.77 percentage points. For VC, ChartAgent likewise excels: the 30B and 235B versions achieve 69.78% and 84.57%, substantially outperforming other chart models and improving over the baselines (66.57% / 82.00%) by 3.21 and 2.57 percentage points. These results indicate that when questions rely more heavily on cross-element alignment and the integration of verifiable visual evidence, tool-integrated reasoning injects low-level perception and measurement capabilities that markedly enhance robustness.

TABLE II
RESULTS ON CHARTQA. ACCURACY (%) ON AUGMENTED (AUG.) AND HUMAN-AUTHORED (HUMAN) QUESTIONS, AS WELL AS THEIR AVERAGE (AVG.), IS REPORTED FOR CHART-SPECIFIC MODELS, GENERAL MLLMs, AND OUR CHARTAGENT.

ChartQA							
Chart Models	Aug.	Human	Avg.	General MLLMs	Aug.	Human	Avg.
MatCha	86.64	37.12	61.88	GPT-4o	85.52	69.52	77.52
UniChart	83.28	34.64	58.96	Gemini-2.5	86.72	78.23	82.45
ChartMoE	90.96	78.32	84.64	Claude4	82.72	76.16	79.44
ChartVLM	82.48	42.08	62.28	Qwen2.5VL-72b	94.35	62.95	78.65
ChartLlama	93.12	58.40	75.76	Qwen3VL-30b	93.20	66.18	79.69
TinyChart	94.48	58.72	76.60	ChartAgent(Qwen3VL-30b)	94.62	75.23	84.92
ChartGemma	90.80	80.16	85.48	Qwen3VL-235b	94.80	77.36	86.08
ChartInstruct	85.04	66.64	75.84	ChartAgent(Qwen3VL-235b)	95.91	83.30	89.61

TABLE III
COMPARISON OF DIFFERENT MODELS ON CHART-TO-TABLE.

Chart Models	RMS _{F1}	General MLLMs	RMS _{F1}
Pix2Struct	78.9	GPT-4o	82.62
UniChart	80.2	Claude-4	90.57
Chartllama	85.8	Gemini2.5	77.98
ChartAss	85.62	Qwen2.5VL	79.82
MatCha	72.45	GPT-4v	81
Deplot	79.64	ChartAgent	91.53

b) *ChartQA*: Table II and Table III present ChartAgent’s performance on various tasks in the ChartQA dataset. For chart question answering (QA), under the large-parameter configuration, ChartAgent attains 95.91% / 83.30% / 89.61% on Aug./Human/Avg., respectively, comprehensively surpassing the baseline; notably, it achieves a substantial +5.94 p.p. gain on the Human subset, which relies more heavily on the alignment and integration of visual evidence. The smaller model, ChartAgent (Qwen3-VL-30B), likewise increases the baseline’s average accuracy from 79.69% to 84.92%. Consistent with the findings in Table I, ChartAgent not only outperforms its size-matched MLLM baselines but also exceeds all other chart-specialized models. For the chart-to-table conversion task, ChartAgent similarly outperforms current MLLMs and several specialized systems such as ChartLlama Han et al. [2023] and ChartAssistant Meng et al. [2024], corroborating its strong capabilities in structured information extraction and integration.

c) *Robustness to Annotation Removal*: To assess the dependence on textual annotations discussed above, we selected 300 chart-question pairs from ChartBench that contain detailed textual labels and conducted experiments with their corresponding de-annotated chart versions. As shown in Fig. 4, in contrast to MLLMs whose accuracy drops sharply after annotation removal, ChartAgent is affected the least. This clearly indicates that ChartAgent substantially reduces its reliance on explicit textual annotations and corroborates its robustness in sparsely annotated settings. This robustness arises from its integrated tool library and verifiable reasoning chain. More detailed visualization results are provided in the Appendix.

TABLE IV
ABLATION ON TOOL LIBRARY, GROUPTALK, AND EIG STRATEGY.

Variant	Acc (%)	Tool Calls
w/o EIG	77.9	8.4
w/o GroupTalk	76.8	5.6
w/o Tool Library	75.4	-
ChartAgent	78.6	6.1

TABLE V
COMBINED EIG SWEEPS ON CHARTBENCH: TOP—COST WEIGHT λ ($B=8$ FIXED); BOTTOM—BUDGET B ($\lambda=0.2$ FIXED).

Param	Value	Acc (%)	Tool Calls
λ	0.0	77.3	9.8
	0.2 (default)	78.6	6.1
	0.5	78.0	5.9
	1.0	76.4	4.3
B	3	73.2	3.0
	5	77.9	4.7
	8 (default)	78.6	6.1
	12	78.8	7.5

C. Ablation Study

a) *Component Ablations*: We conduct ablation studies on the ChartBench subset referenced in IV-B to quantify the contribution of each ChartAgent component (Table IV). The full system attains 78.6% accuracy with an average of 6.1 tool invocations. Removing the EIG-based scheduling strategy reduces accuracy to 77.9% while increasing the average number of tool invocations to 8.4, confirming that an information-gain-driven decision rule effectively suppresses redundant calls and can even improve accuracy under a fixed budget. Eliminating the modular tool library leads to the largest degradation, with accuracy dropping from 78.6% to 75.4%, highlighting its foundational role as the core capability of the system. Removing the GroupTalk module also yields a notable decline (to 76.8%), with an average of 5.6 invocations, close to the full configuration, indicating that cross-expert consensus building and confidence fusion are crucial for harder chart-reasoning cases.

b) *EIG*: We further analyze the behavior of the EIG scheduler (Table V). With the budget fixed at $B = 8$,

increasing the cost weight λ from 0.0 to 0.2 raises accuracy from 77.3% to 78.6% and reduces the average number of tool invocations from 9.8 to 6.1. A large $\lambda = 0.5$ further lowers invocations to 5.9 at a slight accuracy cost (78.0%). When λ becomes too large ($\lambda = 1.0$) the scheduler turns overly conservative, producing only 4.3 invocations on average and causing accuracy to drop to 76.4%.

Fixing $\lambda = 0.2$ and varying the budget B reveals a similar trade-off. An extremely small budget ($B = 3$) severely constrains the agent, yielding 73.2% accuracy with 3.0 tool invocations. Increasing the budget to $B = 5$ and $B = 8$ gradually improves performance to 77.9% and 78.6%, with 4.7 and 6.1 invocations, respectively. Further expanding the budget to $B = 12$ yields only a marginal accuracy gain (78.8%) while incurring higher cost (7.5 invocations). Overall, we adopt $\lambda = 0.2$ and $B = 8$ as the default configuration, which strikes a favorable balance between answer quality and tool-invocation efficiency.

V. CONCLUSIONS

This paper proposes ChartAgent, which reframes chart understanding from an end-to-end black-box mapping into an observable, replayable, and verifiable reasoning chain via TIR, thereby fundamentally reducing MLLMs’ dependence on explicit textual annotations. Leveraging a modular tool library and CEPs, the system remains robust even when key numerical cues are sparse or missing, while maintaining interpretability and trustworthiness. Experimental results show that ChartAgent improves structured understanding and provides a methodological foundation for building trustworthy chart understanding system.

Future work will expand the tool library to cover richer chart elements and geometric relations, and broader application scenarios. For application, we will integrate ChartAgent into a larger-scale scientific agent ecosystem to promote the automated flow from multimodal data to verifiable knowledge, advancing chart understanding from *can do* to *trustworthy*.

REFERENCES

- Josh Achiam, Steven Adler, Sandhini Agarwal, Lama Ahmad, Ilge Akkaya, Florencia Leoni Aleman, Diogo Almeida, Janko Altenschmidt, Sam Altman, Shyamal Anadkat, et al. Gpt-4 technical report. *arXiv preprint arXiv:2303.08774*, 2023.
- Jinze Bai, Shuai Bai, Shusheng Yang, Shijie Wang, Sinan Tan, Peng Wang, Junyang Lin, Chang Zhou, and Jingren Zhou. Qwen-vl: A versatile vision-language model for understanding, localization, text reading, and beyond. *arXiv preprint arXiv:2308.12966*, 2023.
- Shuai Bai, Keqin Chen, Xuejing Liu, Jialin Wang, Wenbin Ge, Sibao Song, Kai Dang, Peng Wang, Shijie Wang, Jun Tang, Humen Zhong, Yuanzhi Zhu, Mingkun Yang, Zhaohai Li, Jianqiang Wan, Pengfei Wang, Wei Ding, Zheren Fu, Yiheng Xu, Jiabo Ye, Xi Zhang, Tianbao Xie, Zesen Cheng, Hang Zhang, Zhibo Yang, Haiyang Xu, and Junyang Lin. Qwen2.5-vl technical report. *arXiv preprint arXiv:2502.13923*, 2025.
- Jinyue Chen, Lingyu Kong, Haoran Wei, Chenglong Liu, Zheng Ge, Liang Zhao, Jianjian Sun, Chunrui Han, and Xiangyu Zhang. Onechart: Purify the chart structural extraction via one auxiliary token. In *Proceedings of the 32nd ACM International Conference on Multimedia*, pages 147–155, 2024.
- Yu Du, Fangyun Wei, and Hongyang Zhang. Anytool: Self-reflective, hierarchical agents for large-scale api calls. *arXiv preprint arXiv:2402.04253*, 2024.
- Tanmay Gupta and Aniruddha Kembhavi. Visual programming: Compositional visual reasoning without training. In *Proceedings of the IEEE/CVF Conference on Computer Vision and Pattern Recognition*, pages 14953–14962, 2023.
- Kai Han, Yunhe Wang, Hanting Chen, Xinghao Chen, Jianyuan Guo, Zhenhua Liu, Yehui Tang, An Xiao, Chunjing Xu, Yixing Xu, et al. A survey on vision transformer. *IEEE Transactions on Pattern Analysis and Machine Intelligence*, 45(1):87–110, 2022.
- Yucheng Han, Chi Zhang, Xin Chen, Xu Yang, Zhibin Wang, Gang Yu, Bin Fu, and Hanwang Zhang. Chartllama: A multimodal llm for chart understanding and generation. *arXiv preprint arXiv:2311.16483*, 2023.
- Kung-Hsiang Huang, Mingyang Zhou, Hou Pong Chan, Yi Fung, Zhenhailong Wang, Lingyu Zhang, Shih-Fu Chang, and Heng Ji. Do lvlms understand charts? analyzing and correcting factual errors in chart captioning. In *Findings of the Association for Computational Linguistics: ACL 2024*, pages 730–749, 2024.
- Kung-Hsiang Huang, Hou Pong Chan, May Fung, Haoyi Qiu, Mingyang Zhou, Shafiq Joty, Shih-Fu Chang, and Heng Ji. From pixels to insights: A survey on automatic chart understanding in the era of large foundation models. *IEEE Transactions on Knowledge and Data Engineering*, 37(5): 2550–2568, 2025a. doi: 10.1109/TKDE.2024.3513320.
- Muye Huang, Lingling Zhang, Jie Ma, Han Lai, Fangzhi Xu, Yifei Li, Wenjun Wu, Yaqiang Wu, and Jun Liu. Charts-ketcher: Reasoning with multimodal feedback and reflection for chart understanding. *arXiv preprint arXiv:2505.19076*, 2025b.
- Aaron Hurst, Adam Lerer, Adam P Goucher, Adam Perelman, Aditya Ramesh, Aidan Clark, AJ Ostrow, Akila Welihinda, Alan Hayes, Alec Radford, et al. Gpt-4o system card. *arXiv preprint arXiv:2410.21276*, 2024.
- Glenn Jocher, Ayush Chaurasia, and Jing Qiu. Ultralytics yolov8, 2023. URL <https://github.com/ultralytics/ultralytics>.
- Rahima Khanam and Muhammad Hussain. Yolov11: An overview of the key architectural enhancements. *arXiv preprint arXiv:2410.17725*, 2024.
- Geewook Kim, Teakgyu Hong, Moonbin Yim, JeongYeon Nam, Jinyoung Park, Jinyeong Yim, Wonseok Hwang, Sangdoon Yun, Dongyoon Han, and Seunghyun Park. Ocr-free document understanding transformer. In *European*

- Conference on Computer Vision*, pages 498–517. Springer, 2022.
- Alexander Kirillov, Eric Mintun, Nikhila Ravi, Hanzi Mao, Chloe Rolland, Laura Gustafson, Tete Xiao, Spencer Whitehead, Alexander C Berg, Wan-Yen Lo, et al. Segment anything. In *Proceedings of the IEEE/CVF International Conference on Computer Vision*, pages 4015–4026, 2023.
- Kenton Lee, Mandar Joshi, Iulia Raluca Turc, Hexiang Hu, Fangyu Liu, Julian Martin Eisenschlos, Urvashi Khandelwal, Peter Shaw, Ming-Wei Chang, and Kristina Toutanova. Pix2struct: Screenshot parsing as pretraining for visual language understanding. In *International Conference on Machine Learning*, pages 18893–18912. PMLR, 2023.
- Heng Lin and Zhongwen Xu. Understanding tool-integrated reasoning. *arXiv preprint arXiv:2508.19201*, 2025.
- Fangyu Liu, Julian Martin Eisenschlos, Francesco Piccinno, Syrine Krichene, Chenxi Pang, Kenton Lee, Mandar Joshi, Wenhui Chen, Nigel Collier, and Yasemin Altun. Deplot: One-shot visual language reasoning by plot-to-table translation. In *The 61st Annual Meeting of The Association for Computational Linguistics*, 2023a.
- Fangyu Liu, Francesco Piccinno, Syrine Krichene, Chenxi Pang, Kenton Lee, Mandar Joshi, Yasemin Altun, Nigel Collier, and Julian Eisenschlos. Matcha: Enhancing visual language pretraining with math reasoning and chart derendering. In *Proceedings of the 61st Annual Meeting of The Association for Computational Linguistics (Volume 1: Long Papers)*, pages 12756–12770, 2023b.
- Fuxiao Liu, Xiaoyang Wang, Wenlin Yao, Jianshu Chen, Kaiqiang Song, Sangwoo Cho, Yaser Yacoob, and Dong Yu. Mmc: Advancing multimodal chart understanding with large-scale instruction tuning. In *Proceedings of the 2024 Conference of the North American Chapter of the Association for Computational Linguistics: Human Language Technologies (Volume 1: Long Papers)*, pages 1287–1310, 2024.
- Haotian Liu, Chunyuan Li, Qingyang Wu, and Yong Jae Lee. Visual instruction tuning. *Advances in Neural Information Processing Systems*, 36:34892–34916, 2023c.
- Ahmed Masry, Xuan Long Do, Jia Qing Tan, Shafiq Joty, and Enamul Hoque. Chartqa: A benchmark for question answering about charts with visual and logical reasoning. In *Findings of the Association for Computational Linguistics: ACL 2022*, pages 2263–2279, 2022.
- Ahmed Masry, Parsa Kavehzadeh, Xuan Long Do, Enamul Hoque, and Shafiq Joty. Unichart: A universal vision-language pretrained model for chart comprehension and reasoning. In *Proceedings of the 2023 Conference on Empirical Methods in Natural Language Processing*, pages 14662–14684, 2023.
- Ahmed Masry, Mehrad Shahmohammadi, Md Rizwan Parvez, Enamul Hoque, and Shafiq Joty. Chartinstruct: Instruction tuning for chart comprehension and reasoning. In *Findings of the Association for Computational Linguistics ACL 2024*, pages 10387–10409, 2024.
- Fanqing Meng, Wenqi Shao, Quanfeng Lu, Peng Gao, Kaipeng Zhang, Yu Qiao, and Ping Luo. Chartassistant: A universal chart multimodal language model via chart-to-table pre-training and multitask instruction tuning. In *In Findings of the Association for Computational Linguistics: ACL2024*, 2024.
- Nikhila Ravi, Valentin Gabeur, Yuan-Ting Hu, Ronghang Hu, Chaitanya Ryali, Tengyu Ma, Haitham Khedr, Roman Rädle, Chloe Rolland, Laura Gustafson, et al. Sam 2: Segment anything in images and videos. *arXiv preprint arXiv:2408.00714*, 2024.
- Ali Salamatian, Amirhossein Abaskohi, Wan-Cyuan Fan, Mir Rayat Imtiaz Hossain, Leonid Sigal, and Giuseppe Carenini. Chartgaze: Enhancing chart understanding in llms with eye-tracking guided attention refinement. In *Proceedings of the 2025 Conference on Empirical Methods in Natural Language Processing*, pages 12104–12124, 2025.
- Timo Schick, Jane Dwivedi-Yu, Roberto Dessì, Roberta Raileanu, Maria Lomeli, Eric Hambro, Luke Zettlemoyer, Nicola Cancedda, and Thomas Scialom. Toolformer: Language models can teach themselves to use tools. *Advances in Neural Information Processing Systems*, 36: 68539–68551, 2023.
- Noam Shazeer, Azalia Mirhoseini, Krzysztof Maziarz, Andy Davis, Quoc Le, Geoffrey Hinton, and Jeff Dean. Outrageously large neural networks: The sparsely-gated mixture-of-experts layer. *arXiv preprint arXiv:1701.06538*, 2017.
- Lingdong Shen, Qigqi, Kun Ding, Gaofeng Meng, and Shiming Xiang. Rethinking comprehensive benchmark for chart understanding: A perspective from scientific literature, 2024.
- Gemini Team, Rohan Anil, Sebastian Borgeaud, Jean-Baptiste Alayrac, Jiahui Yu, Radu Soricut, Johan Schalkwyk, Andrew M Dai, Anja Hauth, Katie Millican, et al. Gemini: a family of highly capable multimodal models. *arXiv preprint arXiv:2312.11805*, 2023.
- Hanchen Wang, Tianfan Fu, Yuanqi Du, Wenhao Gao, Kexin Huang, Ziming Liu, Payal Chandak, Shengchao Liu, Peter Van Katwyk, Andreea Deac, et al. Scientific discovery in the age of artificial intelligence. *Nature*, 620(7972):47–60, 2023.
- Peng Wang, Shuai Bai, Sinan Tan, Shijie Wang, Zhihao Fan, Jinze Bai, Keqin Chen, Xuejing Liu, Jialin Wang, Wenbin Ge, et al. Qwen2-vl: Enhancing vision-language model’s perception of the world at any resolution. *arXiv preprint arXiv:2409.12191*, 2024.
- Xinming Wang, Jian Xu, Aslan H Feng, Yi Chen, Haiyang Guo, Fei Zhu, Yuanqi Shao, Minsi Ren, Hongzhu Yi, Sheng Lian, et al. The hitchhiker’s guide to autonomous research: A survey of scientific agents. *TechRxiv.August 07, 2025*. DOI:10.36227/techrxiv175459840.02185500/V1, 2025.
- Jingxuan Wei, Nan Xu, Junnan Zhu, Gaowei Wu, Qi Chen, Bihui Yu, Lei Wang, et al. Chartmind: A comprehensive benchmark for complex real-world multimodal chart question answering. In *Proceedings of the 2025 Conference on Empirical Methods in Natural Language Processing*, pages 4555–4569, 2025.

- Renqiu Xia, Haoyang Peng, Hancheng Ye, Mingsheng Li, Xiangchao Yan, Peng Ye, Botian Shi, Yu Qiao, Junchi Yan, and Bo Zhang. Structchart: On the schema, metric, and augmentation for visual chart understanding. *arXiv e-prints*, pages arXiv-2309, 2023.
- Zhengzhuo Xu, Sinan Du, Yiyan Qi, Chengjin Xu, Chun Yuan, and Jian Guo. Chartbench: A benchmark for complex visual reasoning in charts. *ArXiv*, abs/2312.15915, 2023. URL <https://api.semanticscholar.org/CorpusID:266550948>.
- Zhengzhuo Xu, Bowen Qu, Yiyan Qi, SiNan Du, Chengjin Xu, Chun Yuan, and Jian Guo. Chartmoe: Mixture of diversely aligned expert connector for chart understanding. In *The Thirteenth International Conference on Learning Representations*, 2024.
- Cheng Yang, Chufan Shi, Yaxin Liu, Bo Shui, Junjie Wang, Mohan Jing, Linran Xu, Xinyu Zhu, Siheng Li, Yuxiang Zhang, et al. Chartmimic: Evaluating lmm’s cross-modal reasoning capability via chart-to-code generation. *arXiv preprint arXiv:2406.09961*, 2024.
- Shunyu Yao, Jeffrey Zhao, Dian Yu, Nan Du, Izhak Shafran, Karthik R Narasimhan, and Yuan Cao. React: Synergizing reasoning and acting in language models. In *The Eleventh International Conference on Learning Representations*, 2022.
- Liang Zhang, Anwen Hu, Haiyang Xu, Ming Yan, Yichen Xu, Qin Jin, Ji Zhang, and Fei Huang. Tinchart: Efficient chart understanding with program-of-thoughts learning and visual token merging. In *Proceedings of the 2024 Conference on Empirical Methods in Natural Language Processing*, pages 1882–1898, 2024.

APPENDIX

To overcome the limitations of current multimodal large language models (MLLMs) in fine-grained visual measurement and traceable reasoning, we develop a modular tool library covering more than a dozen core capabilities. Detailed tool names and descriptions are provided in Table VI

By coupling low-level visual perception with high-level logical reasoning, this library endows the agent with chart-analysis abilities comparable to those of a human analyst. At the perception layer, we train a dedicated YOLO-based `KeyElement Tool` to precisely localize the plot area, axes and ticks, legends, and data elements (e.g., bars) from unstructured bitmap images; its outputs not only provide spatial priors for subsequent geometric computations but also bridge the pixel and semantic spaces. The `Curve Detection Tool`, operating in the HSV color space with multi-channel thresholding and skeletonization, extracts clean topological skeletons that capture trend information from complex backgrounds. Meanwhile, textual content serves as a crucial semantic anchor for chart understanding. To this end, we integrate a Qwen-VL-OCR engine as `OCR Tool` that leverages the multimodal representation capacity of MLLM to jointly extract text content and its precise bounding boxes with confidence scores, thereby improving robustness to rotated text, dense numeric labels, and special symbols, and enabling reliable alignment between numeric values and textual annotations. Several visualization results of these tools are shown in the fig 5.

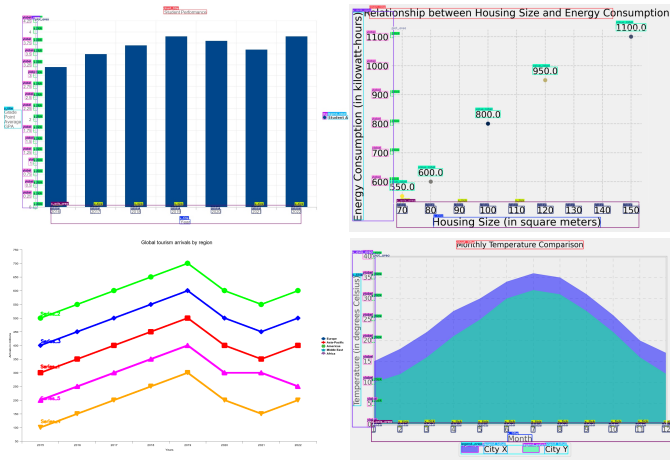


Fig. 5. Low-level perception visualization results.

To accommodate different data-encoding paradigms, the tool library further incorporates specialized high-level measurement modules. For pie and donut charts, where values are expressed through area proportions, we introduce the `AugmentSegmentation Tool` following a segment-cluster-quantify pipeline: SAM’s zero-shot segmentation is first employed, using chart-type-aware prompts (e.g., a single center point for solid pies, a combination of center-negative points and bounding-box prompts for donut charts) to extract the main region. Next, valid pixels are sampled in the HSV/RGB color spaces, and K-Means clustering is applied

to automatically group dominant color clusters while filtering anti-aliasing noise. Finally, the pixel proportion of each cluster is computed to infer the underlying data distribution.

For Cartesian-coordinate charts such as line and bar charts, we design an `AuxLine Tool` that mimics the human auxiliary-line projection strategy. Leveraging intermediate outputs from detection modules, the tool builds a calibration function between pixel coordinates and numeric values via linear regression. Using x-axis ticks as anchors, auxiliary lines are projected toward the y-axis to locate geometric intersections between projection paths and data skeletons; the calibration model then maps intersection pixel coordinates back into precise numerical values, enabling a reliable conversion from image-level measurements to structured data. Visualization results for the above tools are shown in the fig. 6.

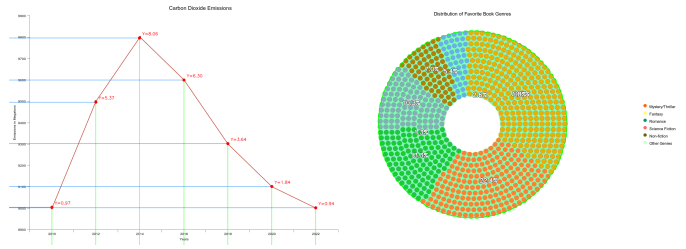


Fig. 6. High-level perception visualization results.

After obtaining accurate structured visual evidence, the Reasoning Tools undertake high-level analysis and result consolidation. The workflow typically begins with a `Classification Tool` to guide subsequent orchestration. A `Relational Reasoning Tool` constructs semantic and spatial relation graphs among chart elements, while `Numerical Calculation Tool` perform ratio conversions, summations, and other arithmetic operations to mitigate the inherent computational limitations of language models. Finally, a `Data Structuring Tool` aggregates OCR text, detection boxes, auxiliary-line readings, and clustering outputs into a standardized table or JSON-based Evidence Package, achieving a tightly coupled integration of low-level perception and high-level reasoning. This pipeline enables transparent and verifiable automated analysis of complex charts.

Fig. 7, fig. 8, and fig. 9 illustrate the intermediate visual outputs of ChartAgent on three common chart types—bar charts, line charts, and pie/sector charts—using samples drawn from the ChartBench test set. Fig. 7 presents the complete analysis pipeline for a bar chart: (a) shows the original image; (b) displays the intermediate results after key-element detection; and (c) illustrates the extraction of individual bars using the segmentation tool. Based on the information from (b) and (c), the system then draws auxiliary lines and performs numerical reading. The textual annotations beside the auxiliary lines denote relative tick counts (measured in units of the y -axis ticks). For the query “According to this chart, what is the Number of Cars Sold of Hyundai?”, the ground-truth value is 4.5. ChartAgent first estimates that the bar corresponding to Hyundai spans approximately 9.1 tick intervals, and

TABLE VI
OVERVIEW OF TOOL LIBRARY

Type	Tools	Brief Explanation
Visual perception tools	Segmentation Tool	Used to precisely isolate specific regions or objects (like legend items, bar segments, or pie slices) from the chart background, providing clean input for subsequent recognition and measurement.
	AugmentSegmentation Tool	Performs instance segmentation on the chart image to precisely isolate and identify every individual element. Following segmentation, it calculates the pixel ratio or area percentage occupied by each distinct instance relative to the data area or the entire chart, allowing for proportional analysis.
	AuxLine Tool	Automatically generates and projects horizontal or vertical aux-lines onto the chart, used to pinpoint the axis values corresponding to data points for accurate numerical reading or comparison.
	KeyElement Detection	Specifically identifies and localizes the core components of the chart, such as the title, axis labels, data area, legends, and tables, serving as the starting point for structural chart understanding.
	Curve Detection	Focuses on recognizing and tracking data curves or trend lines in line charts, scatter plots, etc., to extract discrete data points or analyze the change trajectory.
	OCR Tool	Processes all textual information in the chart image, including axis tick values, titles, legend text, and data labels, converting image-based text into processable strings.
	Color Matching Tool	Responsible for associating the visual elements in the data area (bars or curves) with the colors and labels defined in the legend, thereby determining each data series' meaning.
Reasoning tools	Classification Tool	Used to identify the overall chart type .
	Numerical Calculation Tool	Executes fundamental mathematical operations and logical inferences .
	Data Structuring Tool	Organizes OCR, detection, and numerical results into a standard table or JSON format , enabling structured queries and analysis.
	Relational Reasoning Tool	Analyzes semantic and spatial relationships between chart elements , constructing a logical graph from segmentation and detection results.

since each interval represents 0.5 units, the system computes $9.1 \times 0.5 \approx 4.55$, which aligns closely with the true value.

Fig. 8 demonstrates the reasoning process and key intermediate artifacts for a line chart following the same workflow. Fig. 9 presents a sector-chart example: by sequentially invoking the segmentation tool and the enhanced AugmentSegmentation module, ChartAgent robustly performs sector instantiation and proportion estimation, effectively addressing visual-measurement scenarios that conventional MLLMs struggle to handle.

Fig. 10 presents several representative failure cases. In (a), the donut chart is incorrectly analyzed: unlike conventional charts with solid color fills, this example is composed of dense dotted patterns. While the primary segmentation stage remains largely correct, the enhanced segmentation procedure (segment-cluster-quantify) is adversely affected by boundary noise and color mixing introduced by the dot-matrix texture. This results in inaccurate sector instantiation and area estimation, and in some cases triggers over-segmentation or under-segmentation.

(b) shows an uncommon 3D bar chart. The auxiliary-line tool assumes a two-dimensional orthographic projection and does not model perspective or occlusion effects. Consequently, the system directly maps the visually observed 3D bar heights

to numeric values, leading to systematic underestimation or overestimation.

Algorithm 1 details the inference procedure of *ChartAgent* under a Think–Observe–Execute paradigm with an explicit computation budget. Lines 1–3 initialize the step index, the cumulative cost, the interaction history \mathcal{H}_0 , and the evidence package \mathcal{E}_0 . The main loop (lines 6–20) is executed while the accumulated cost C remains below the budget B . At each iteration, ChartAgent selects an action a_t from the tool library \mathcal{T} or a special `<finish>` action (line 8) by maximizing a cost–benefit objective, where the expected information gain $EIG(a | \mathcal{H}_t)$ is penalized by the tool cost $c(a)$ weighted by λ . The loop is terminated if the `finish` action is chosen or if the expected information gain of the best action falls below a threshold η (lines 10–12), thereby preventing uninformative or redundant tool calls. Whenever a tool is executed (lines 14–19), its output z_t is appended to the evidence package \mathcal{E}_{t+1} and the history state \mathcal{H}_{t+1} is updated via `UpdateState`, while the cumulative cost and step index are incremented accordingly.

Upon termination of the Think–Observe–Execute loop, ChartAgent proceeds to a reflection phase driven by multi-expert collaboration (lines 22–24). In this stage, the procedure `GroupTalk` takes as input the chart image x , the user

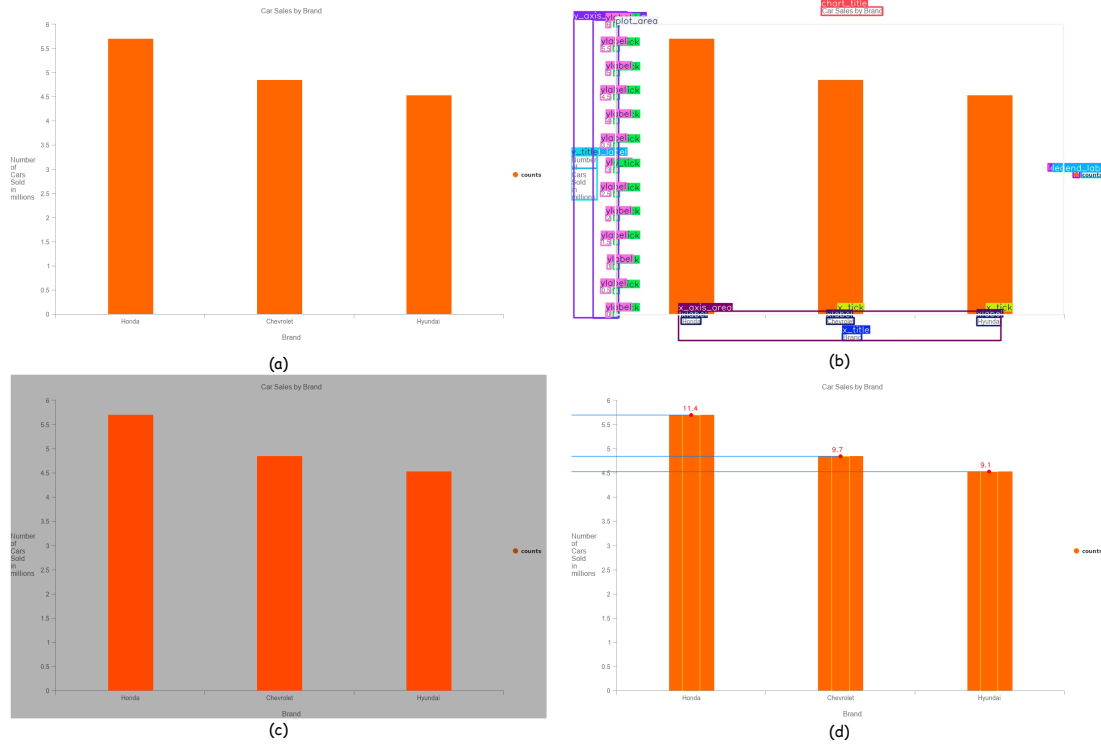


Fig. 7. A typical successful case for bar chart.

query q , the final history \mathcal{H}_t , and the evidence package \mathcal{E}_t to obtain a set of expert votes, denoted as $Votes$. These votes encode the independent assessments of multiple specialized expert modules conditioned on the same collection of intermediate reasoning steps and tool outputs. The function `AggregateAndCalibrate` then fuses and calibrates these votes to produce the final answer y , which is returned together with the final evidence package \mathcal{E}_t . This two-stage design—cost-aware iterative evidence acquisition followed by collaborative reflection—enables `ChartAgent` to balance computational efficiency, predictive accuracy, and interpretability in chart understanding tasks. Shen et al. [2024]

Algorithm 1: ChartAgent Inference Framework

Input: Chart image x ; user instruction q ; tool library \mathcal{T} ; budget B .
Output: Final answer y ; evidence package \mathcal{E} .

```

// Initialization
1  $t \leftarrow 0$ ;  $C \leftarrow 0$  // Step index and current cost
2  $\mathcal{H}_0 \leftarrow \emptyset$ ;  $\mathcal{E}_0 \leftarrow \emptyset$  // History and evidence
// Think-Observe-Execute loop
3 while  $C < B$  do
    // Select action via cost--gain trade-off
4    $a_t \leftarrow \arg \max_{a \in \mathcal{T} \cup \{\text{finish}\}} (\text{EIG}(a \mid \mathcal{H}_t) - \lambda \cdot c(a))$ 
5   if  $a_t = \text{finish}$  or  $\text{EIG}(a_t) \leq \eta$  then
6     break
    // Execute tool and update evidence
7    $z_t \leftarrow \text{Execute}(a_t, x, \mathcal{H}_t)$ 
8    $\mathcal{E}_{t+1} \leftarrow \mathcal{E}_t \cup \{(a_t, z_t)\}$ 
9    $\mathcal{H}_{t+1} \leftarrow \text{UpdateState}(\mathcal{H}_t, z_t)$ 
10   $C \leftarrow C + c(a_t)$ 
11   $t \leftarrow t + 1$ 

// Reflect: multi-expert collaboration
12  $Votes \leftarrow \text{GroupTalk}(x, q, \mathcal{H}_t, \mathcal{E}_t)$ 
13  $y \leftarrow \text{AggregateAndCalibrate}(Votes)$ 
14 return  $y, \mathcal{E}_t$ 

```

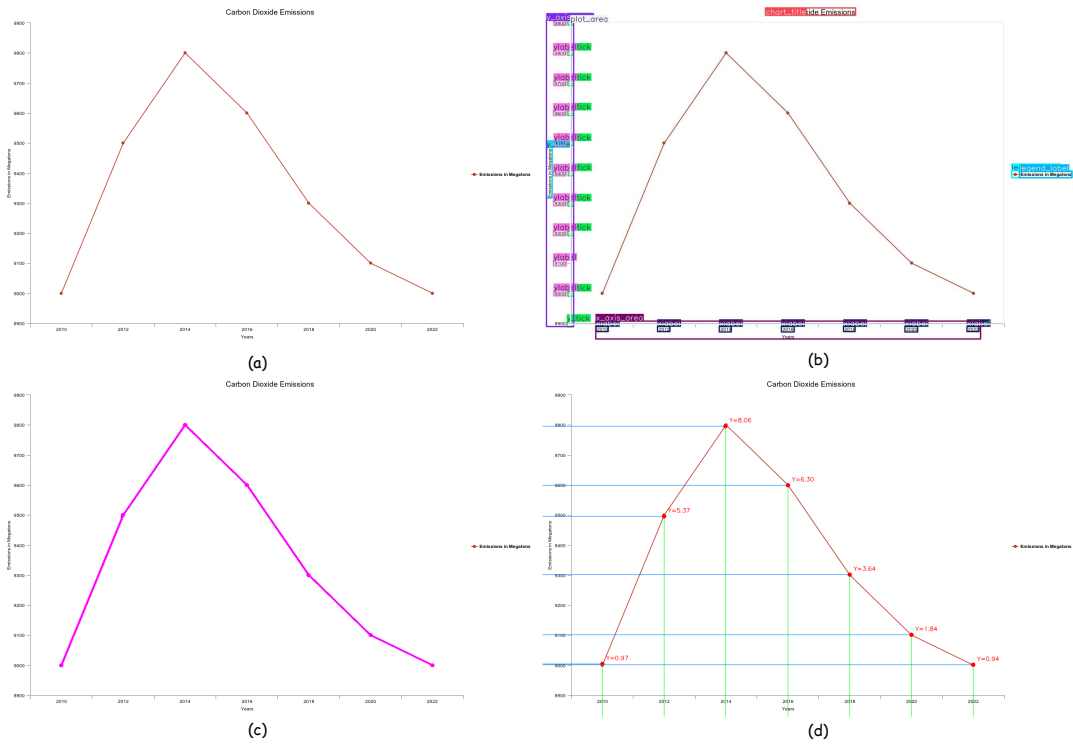


Fig. 8. A typical successful case for line chart.

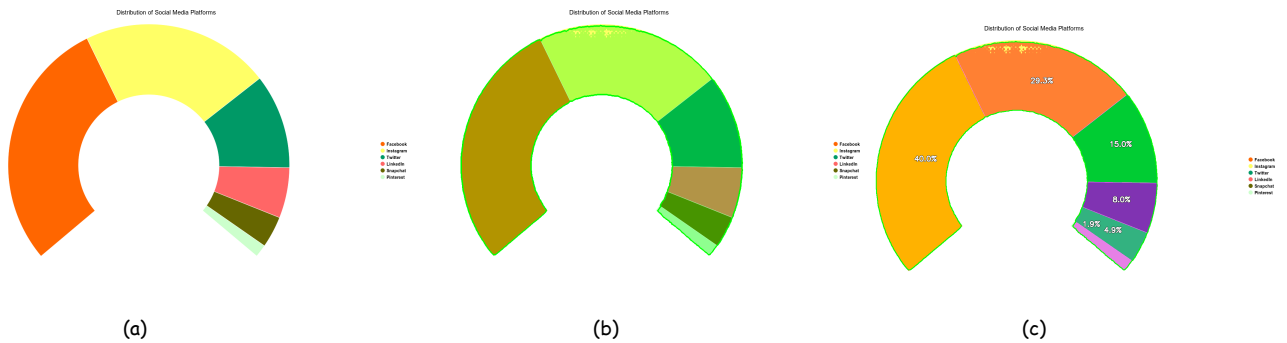


Fig. 9. A typical successful case for sector charts.

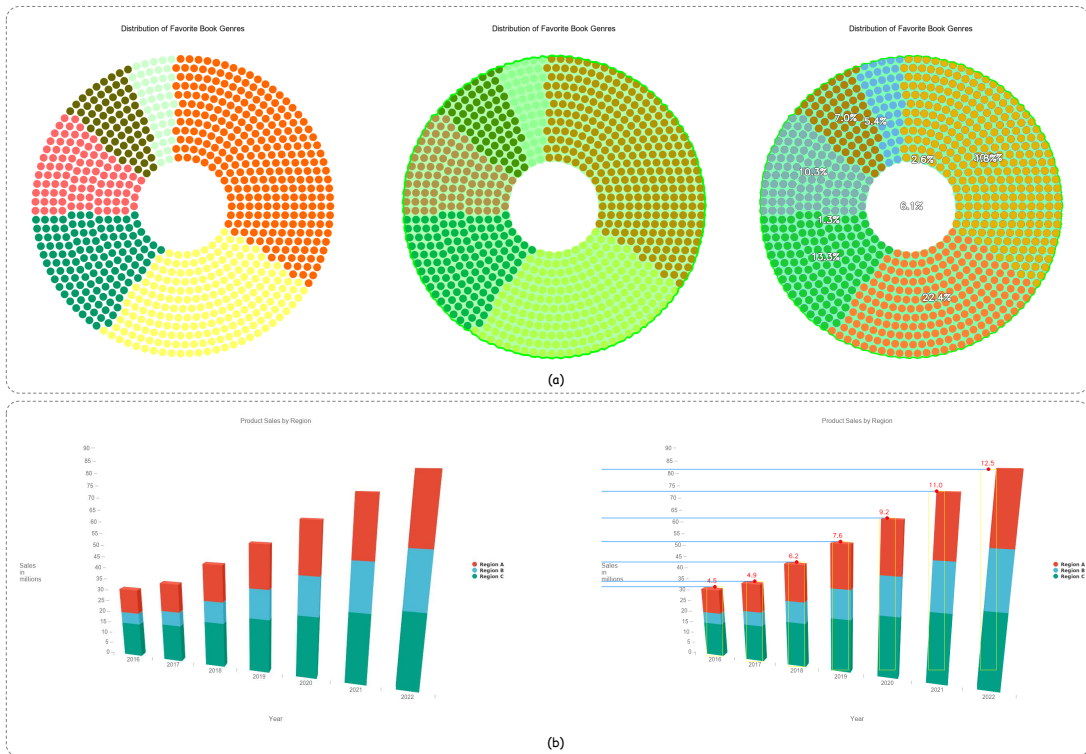


Fig. 10. Some failure cases.

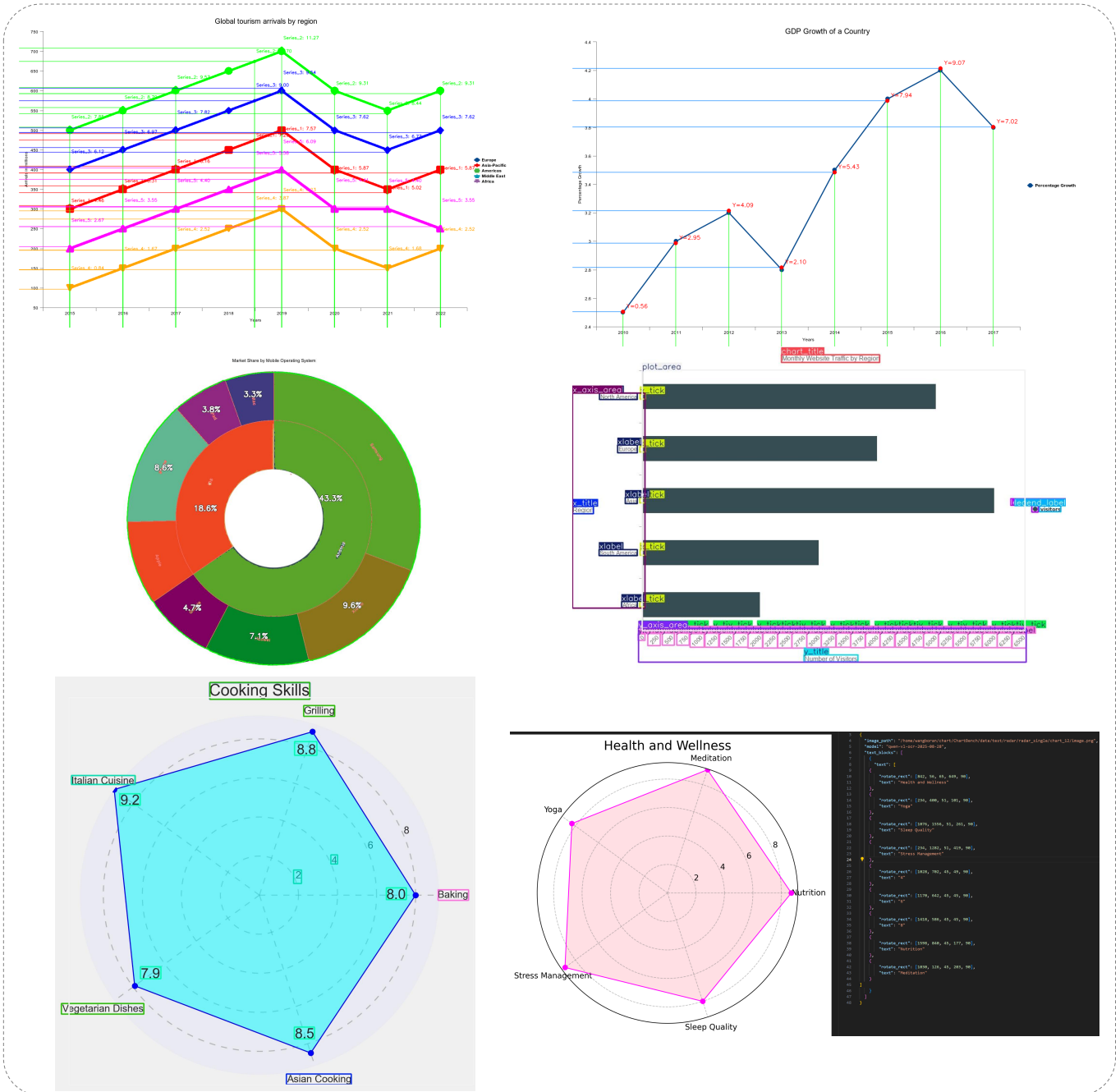


Fig. 11. Several representative examples of CEP.